Int J Adv Manuf Technol (2012) 61:1043–1055
DOI 10.1007/s00170-011-3758-8

ORIGINAL ARTICLE

Composite fabrication using friction stir processing—a review

H. S. Arora · H. Singh · B. K. Dhindaw

Received: 7 March 2011 / Accepted: 7 November 2011 / Published online: 4 December 2011

Abstract Composite manufacturing is one of the most imperative advances in the history of materials. Nanoparticles have been attracting increasing attention in the composite community because of their capability of improving the mechanical and physical properties of traditional fiber-reinforced composites. Friction stir processing (FSP) has successfully evolved as an alternative technique of fabricating metal matrix composites. The FSP technology has recently shown a significant presence in generation of ex situ and in situ nanocomposites. This review article essentially describes the current status of the FSP technology in the field of composite fabrication with the main impetus on aluminum and magnesium alloys.

Keywords Friction stir processing · Nanocomposites · Aluminum and magnesium alloys

1 Introduction

The development of composite materials and the related design and manufacturing technologies is one of the most important advances in the history of materials. Composites are multifunctional materials having unprecedented mechanical and physical properties that can be tailored to meet the requirements of a particular application. The unique characteristics of composites provide the engineer with design opportunities not possible with conventional monolithic (unreinforced) materials. Many manufacturing processes for composites are well adapted to the fabrication of large, complex structures. This allows consolidation of parts, which can reduce manufacturing costs [1]. The newness and unconventional nature of composites have undoubtedly brought in their own peculiarities and complexities in design, analysis, and fabrication. However, the current advances in processing technology coupled with advanced computational technology and numerical methods have played a key role in overcoming such difficulties and promote the application and growth of composites [2].

Particle-reinforced metal matrix composites (MMCs) have many advantages such as enhanced modulus and strength. They have been produced mainly via powder metallurgy (P/M) route or molten metal processing [3]. With P/M processing, the composition of the matrix and the type of reinforcement can be varied with little limitations. In P/M route, the matrix alloy powder is blended with reinforcement particles to achieve homogeneous mixture. Secondary processing methods, such as extrusion and rolling, are essential in processing composites produced by P/M route, since they are required to consolidate the composite fully. Normally, a high extrusion is required to disrupt the oxide film between metal powder particles, and it also improves the distribution of reinforcement. A possible alternative is to synthesize the reinforcement in situ in the metal matrix [4].

After the inception, success and gradually wider applications of the friction stir welding technique developed by "The Welding Institute" in UK [5], its recent modification into friction stir processing (FSP) [6, 7] has also attracted attention. FSP has been demonstrated to be an effective means of refining the grain size of cast or wrought aluminum-based alloys via dynamic recrystallization. A fine grain size typically in the range of 0.5–5 μm in the dynamically recrystallized zone of friction stir-processed

H. S. Arora (✉) · H. Singh · B. K. Dhindaw
School of Mechanical, Material and Energy Engineering,
Indian Institute of Technology Ropar,
Rupnagar, Punjab 140001, India
e-mail: harpreetsa@iitrpr.ac.in

(FSPed) aluminum and magnesium alloys has been widely reported [6–10]. Extrafine grain sizes in the range of 30–180 nm have also been demonstrated [11]. There are several methods to fabricate particulate reinforced Al or Mg-based composites, including stir casting [12], squeeze casting [13], molten metal infiltration [14], and P/M [15]. FSP appears to offer another route to incorporate ceramic particles into the metal matrix to form bulk composites. The severe plastic deformation and material flow in stirred zone (SZ) during FSP can be utilized to achieve bulk alloy modification via mixing of other elements or second phases into the stirred alloys. As a result, the stirred material becomes an MMC or an intermetallic alloy with much higher hardness and wear resistance. Recently, FSP has been applied successfully to produce Al–Al_2Cu in situ composite from Al–Cu elemental powder mixtures [16], Al–$Al_{13}Fe_4$ in situ nanocomposite from Al–Fe elemental powder mixtures [17], and Al–Al_3Ti nanocomposite from Al–Ti elemental powder blends [18].

The purpose of this article is to review the current state of FSP technology in the field of fabrication of ex situ and in situ composites. The study is divided into two sections. The first section gives some recent studies related to composite fabrication using FSP, and the second section focuses on nanocomposites using FSP. This division has been done because of the difference of strengthening mechanisms operating at the micron and submicron/nano-level; for example, it is believed that the contribution of the famous Orowan strengthening mechanism to overall strength of the material became considerably higher when the particle size in the material matrix approaches to submicron/nanolevel as compared with the case when the particle are in micron size range. Similarly, grain structure is believed to be much stable in the presence of fine submicron-sized precipitate particles uniformly distributed in the entire material matrix. The fine precipitate particles in the material matrix also aid in the evolution of finer-grain structure during thermomechanical processing of the material through particle pinning, which also aids in material strengthening through grain boundary strengthening.

The contribution of these mechanisms is not so prominent when the particles are in micron size range. A comparative study in a tabular format is also provided for immediate reference.

2 Fabrication of composites

Metal matrix composites (MMCs) are an important class of material for structural and electrical applications [19]. Particulate-reinforced MMCs are of particular interest because of their easy fabrication, low cost, and isotropic properties. In conventionally processed powder metallurgy composites, the reinforcing particles are formed prior to their addition to the matrix metal. In this case, the scale of reinforcing phase is limited by the starting powder size, which is typically of the order of several to tens of micrometers and rarely below 1 μm. Other drawbacks of conventionally processed MMCs that are required to be overcome are poor interfacial bonding and poor wettability between the reinforcement and the matrix due to surface contamination of the reinforcements. It is widely recognized that the mechanical properties of MMCs are controlled by the size and volume fraction of the reinforcements as well as the nature of the matrix–reinforcement interface [20]. It is possible to produce surface composite layer by FSP process as well [4]

Wang et al. [21] produced bulk SiC-reinforced aluminum MMCs by FSP. Commercial SiC powder and 5A06Al (in Chinese standard) rolled plate were used in this test. A groove was prepared at the edge of pin in the advancing side, which had 0.5-mm width and 1.0-mm depth. The groove was 2.8 mm far from the center line, and the SiC powder was deposited into it before processing. The FSP tool was made of high-speed steel and had a columnar shape shoulder and a screwed pin. The tool penetrated into the plate until the shoulder's head face reached 0.5 mm under upper surface. The rotational speed of tool was 1,180 rpm, and the travel speed was 95 mm/min along the center line. The distribution of fabricated MMCs did not limit to surface composites under the tool shoulder. The SiC powder could flow beyond the thermomechanical affected zone (TMAZ) under the tool shoulder, and it covered the range of 1.5 mm apart from the edge of the pin at the advancing side. However, the width became narrower in deeper position, and the distribution of MMCs was about 2.5 mm at the depth of 2 mm, which was in the range of pin at the advancing side. The microhardness of base metal was about 88 HV. On the depth of 0.5 and 1.0 mm under surface, the microhardness was steady, 10% higher than the base metal, due to integral dispersed SiC.

Synthesis of multiwalled carbon nanotube (CNT)-reinforced aluminum alloy composite was done by Lim et al. [22] via FSP. The composite materials were synthesized by encasing the multiwalled CNT powder in a 0.3-mm×2.3-mm groove in a lower plate, which was covered by a top sheet before FSP, as shown in Fig. 1a. A sheet of 1.1-mm-thick Al 6111–T4 alloy was used as cover plate to contain the CNT material within the groove during processing, and the lower plate was 6.35-mm-thick Al 7075–T6 alloy. The CNT-based material had outer diameters of 30–50 nm and had a length of 10–20 μm (Fig. 1b). All samples were processed using a tool that consists of a 10-mm-diameter shoulder and a 4-mm diameter and 2.2-

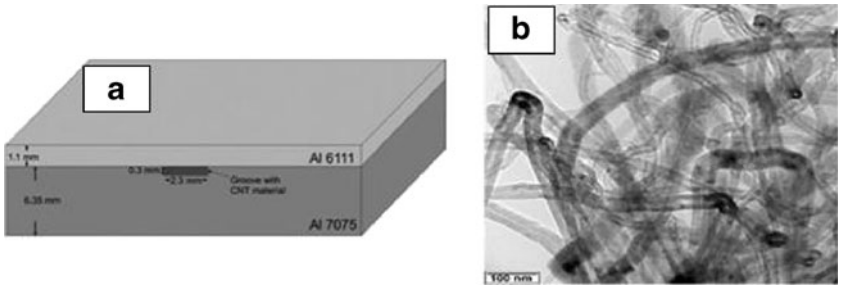

Fig. 1 (**a**) Schematic diagram of base material layout prior to FSP. (**b**) TEM micrograph of the MWCNT material [22]

mm-long pin, with a M4 metric thread profile. The rotational speed used ranged from 1,500 to 2,500 rpm, and the linear speed was 2.5 mm/s. The shoulder penetrated into the upper sheet of Al 6111 by 0.03–0.24 mm. It was observed that when a tool rotation speed of 1,500 rpm was used and the shoulder penetration depth (PD) was increased to 0.24 mm, the stir zone was free of voids and comprised of lamellae of intermixed layers of Al 6111 and Al 7075 material. Increasing the tool rotation speed to 2,500 rpm and the shoulder PD to 0.24 mm reduced the thickness of the lamellae. Scanning electron microscope (SEM) and transmission electron microscope (TEM) confirmed that nanotubes were embedded in the lamellae regions of the Al-alloy stir zone and that their multiwalled structure was retained; however, evidence was observed that the nanotubes may have fractured during FSP. It was found that increasing the tool rotation speed from 1,500 and 2,500 rpm and increasing the tool shoulder PD improved the distribution of nanotubes in the Al-alloy matrix. A completely uniform distribution could not be achieved when regularly tangled nanotubes were used as the base material, and it was suggested that multiple passes may be required to further improve the dispersion of nanotubes in the matrix.

Ke et al. [23] produced in situ Al–Ni intermetallic composites using FSP. The materials used were pure aluminum plate (99.6% purity, 5-mm thickness) and pure nickel powder (99.0% purity, 2.3 μm). The nickel powder was filled into two rank holes (2.5 mm in diameter and 3 mm in depth), with an interval of 3 mm on two matrix plates before FSP. The FSP tool had a columnar shape (Ø28 mm) with a screw thread probe (M10 mm, 8.5 mm in length). The tool penetrated into the plate until the shoulder's head face reached 0.4–0.5 mm under upper surface. The constant tool rotating rate of 1,500 rpm, a travel speed of 23.5 mm/min, and a tool tilt angle of 3° were used. Three FSP passes were applied to enhance the Al–Ni reaction. Defect-free Al–Ni intermetallic composites were successfully produced by three-pass FSP and with a subsequent heat treatment at 550°C for 6 h. Al_3Ni and Al_3Ni_2 existed in the processing zone, and the particles were found to have good bonding with the matrix. After three-pass FSP, the grain refinement and the precipitation hardening effect of the Al_3Ni intermetallics resulted in a significant increase in the microhardness and tensile strength of the Al–Al_3Ni composites. The microhardness for the Al_3Ni_2 and Al_3Ni intermetallics was measured as 1,283 and 841 HV, respectively, and the ultimate strength of the composite was measured as 144 MPa.

Properties of FSPed Al 1100–NiTi composite were analyzed by Dixit et al. [24]. Four small holes, 1.6 mm in diameter and 76 mm in length, were drilled at about 0.9 mm below the surface in Al 1100 plates. NiTi powders with particles in the size range of 2–193 μm were trapped inside the holes. The powder-filled plates were then subjected to FSP at 1,000 rpm, 25-mm/min linear speed, and a plunge depth of 2.3 mm. From the FSPed composites, three sets were prepared. While the first set was kept in the as- FSPed condition, the other samples were subjected to liquid nitrogen temperatures and given a cold rolling reduction of 38% in thickness. From these samples, some were preserved in the cold-rolled condition, while a third set was prepared by heating and annealing the cold-rolled samples at 85°C for 15 min. The combination of cold rolling and annealing was performed to induce the phase transformations in NiTi that would help to originate residual stresses in the matrix. It was observed that FSP could be used to prepare composites successfully. The embedded particles were uniformly distributed and had strong bonding with the matrix, and no interfacial products were formed during the processing. With adequate processing, the shape memory effect of NiTi particles could be used to induce residual compressive and tensile stresses in the parent matrix. Both the experimental and the modeled values showed improved mechanical properties in the prepared composite in the form of enhanced modulus, yield strength (YS), and microhardness values.

SiC-reinforced AZ91composite was prepared by Asadi et al. [25] by using FSP. AZ91/SiC surface composite layer was fabricated using the 5 μm SiC powders as reinforcing particles and as-cast AZ91 as matrix. The thickness of the plate was 5 mm. A steel tool with a square pin, 5 mm in diameter and 2.5 mm in length, and with 15-mm–diameter shoulder was used. The tool rotational and linear speeds

were changed from 710 to 1,400 rpm and 12.5 to 80 mm/min, respectively. The tool tilt angles used were 2.5°, 3°, 3.5°, and 4°, and PD was changed from 0.15 to 0.45 mm. The microstructure evaluation of the FSPed zone and the distribution of the SiC particles in SZ were carried out by optical and scanning electron microscopy. Energy dispersive spectroscopy composition analysis was performed to obtain the composition of the different regions of specimen section. Microhardness of the specimens was measured in 1-mm distance from the upper surface in the cross section using a Vickers microhardness testing machine. In all the tests, a load of 200 g was applied for 15 s. It was found that decreasing the rotational speed and increasing the linear speed led to a decrease in the grain size. PD was found to be an effective parameter to produce a sound surface layer, and its value was found to be influenced by linear speed, rotational speed, and tilt angle value. The grain size reduced from 150 to 7.17 μm, and stir zone hardness increased from 63 to 96 HV.

Mahmoud et al. [26] studied the wear characteristics of surface-hybrid-MMCs layer fabricated on an aluminum plate using FSP. Commercially available pure aluminum Al-1050-H24 plates of 5-mm thickness were used as the base material. Mixtures of SiC and Al_2O_3 particles in different ratios were used as the reinforcements. The wear behavior of the surface metal matrix composites (SMMCs) was evaluated by using a ball-on-disk tester in air at room temperatures. It was observed that the reinforcement particles (SiC, Al_2O_3, or their mixture) were distributed almost homogenously over the nugget zone by FSP without any defects, except some small voids forming around the Al_2O_3 particles. The average hardness of the resulted composites increased to about 60 HV at 100% SiC (almost three times that of the nugget zone without reinforcement), and it decreased with an increase in relative ratio of Al_2O_3 particles. The average friction coefficient values exhibited general tendency to decrease with increasing the relative content of Al_2O_3. It was found that the addition of reinforcement powder (SiC, Al_2O_3, or mixture) to an aluminum matrix was beneficial in reducing the wear volume loss, especially at relatively low loads.

Microstructure and tribological performance of an aluminum alloy-based hybrid composite produced by FSP were investigated by Alidokht et al. [27]. The material used in this study was cast A356 plates with SiC powder (99.5% pure and 30-μm average particle size) and MoS_2 powder (99% pure and 5-μm average particle size). The FSP parameters were kept constant at 1,600 rpm, and 50 mm/min. To insert the powders, a groove with a depth and width of 3.5 and 0.6 mm, respectively, was machined out of the cast A356 work pieces. The dry wear tests were conducted with a pin-on-disk Tribometer. Figure 2a shows the SEM image of SiC and MoS_2 particle dispersion in the stir zone. In this micrograph, the dark particles are SiC,

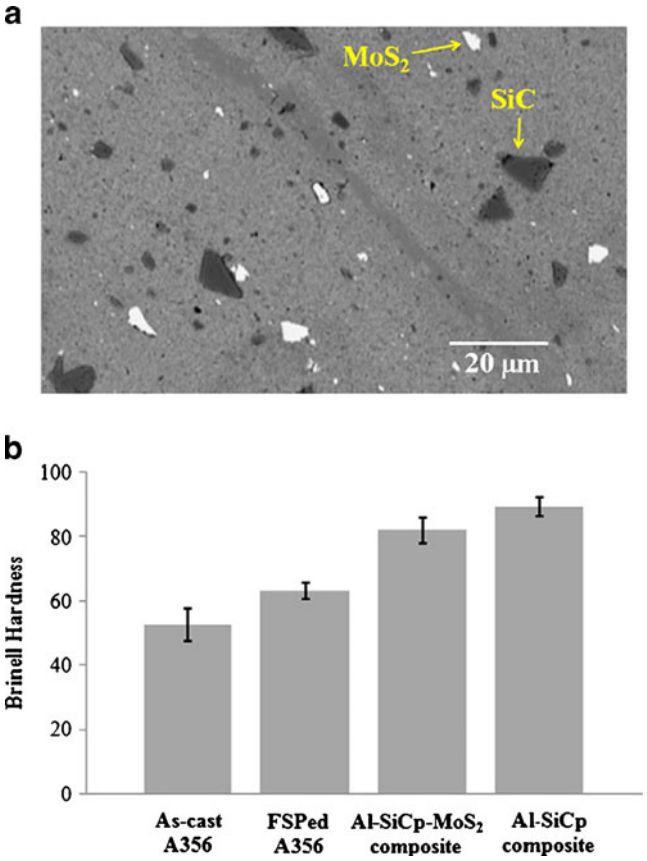

Fig. 2 (**a**) SEM image of particle dispersion in hybrid composite produced by FSP. (**b**) Variation of Brinell hardness in as-cast, FSPed A356 and composite samples [27]

whereas the brighter particles are MoS_2. The average size of the SiC at the stir zone is estimated to be 10 μm. This is significantly smaller than that in the as-received SiC powder (30 μm). Figure 2b indicates the variations of hardness in the as-cast A356 and as-processed samples. Hardness test revealed that the FSPed A356 displays higher hardness compared with the as-cast A356. It was found that both the extent of wear and wear rate were significantly lower in the FSPed A356 and composite samples as compared with the as-cast A356. Furthermore, surface hybrid composite offered the maximum resistance to wear. Detailed examination of the wear track of the FSPed A356 sample revealed features associated with adhesive and abrasive mechanisms, and it was observed that the extent of adhesive and abrasive wear decreased in FSPed A356 due to a comparatively lower coefficient of friction and higher hardness, respectively. It was proposed that formation of mechanically mixed layer separate the wearing surfaces and reduced the wear rate. It was concluded that although the A356/SiC composite had the highest hardness, the unstable mechanically mixed layer in the absence of the lubricant phase led to lower wear resistance as compared with the hybrid composite. The depth of

subsurface deformation in the hybrid composite was found to be distinctly less than the SiC-reinforced MoS_2-free composite.

Summary of the investigations on composite fabrication using FSP is given in Table 1.

3 Fabrication of nanocomposites

In recent years, nanoparticles have been attracting increasing attention in the composite community because of their capability of improving the mechanical and physical properties of traditional fiber-reinforced composites [28–31]. Their nanometer size, leading to high specific surface areas of up to more than 1,000 m^2/g, and extraordinary mechanical, electrical, and thermal properties make them unique nanofillers for structural and multifunctional composites. Commonly used nanoparticles in nanocomposites include multiwalled nanotubes, single-walled nanotubes, carbon nanofibers, montmorillonite, and nanoclays. Other nanoparticles such as SiO_2, Al_2O_3, TiO_2, and nanosilica are also used in the nanocomposites [32]. FSP provides one of the alternatives of generating in situ nanocomposites resulting in superior mechanical properties caused by fine and stable reinforcements with good interfacial bonding dispersed uniformly in the matrix. The next section

Table 1 Summary of the investigations on composite fabrication using FSP

Investigator name	Material investigated	Characteristic studied	Prominent results
Wang et al. [21]	Aluminum alloy 5A06Al (in Chinese standard) and SiC powder	Microhardness of the MMC formed	• The SiCp could flow beyond the TMAZ under the tool shoulder, and it covered the range of 1.5 mm apart from the edge of the pin at the advancing side. • On the depth of 0.5 and 1.0 mm under surface, the microhardness was steady, 10% higher than the base metal, due to integral dispersed SiC
Lim et al. [22]	Aluminum alloys 6111–T4 and 7075–T6 and MWCNTs	Effect of processing parameters on distribution of MWCNTs in the composite formed	• At a tool rotation speed of 1,500 rpm and a shoulder penetration depth of 0.24 mm, the stir zone was free of voids. • Increasing the tool rotation speed to 2,500 rpm and the shoulder penetration depth to 0.24 mm reduced the thickness of the lamellae. • It was suggested that multiple passes might be required to further improve the dispersion of nanotubes in the matrix.
Ke et al. [23]	Pure aluminum plate and pure nickel powder	Microhardness and tensile strength	• After 3-pass FSP, the grain refinement and the precipitation hardening effect of the Al_3Ni intermetallics resulted in a significant increase in the microhardness and tensile strength of the Al– Al_3Ni composites.
Dixit et al. [24]	Aluminum alloy 1100 and NiTi powder	Mechanical properties of the composite formed	• The embedded particles were uniformly distributed and had strong bonding with the matrix, and no interfacial products were formed during the processing. • Both the experimental and the modeled values showed improved mechanical properties in the prepared composite in the form of enhanced modulus, yield strength, and microhardness values
Asadi et al. [25]	Magnesium alloy AZ91 and SiC powder	Microstructure evaluation of the FSPed zone and the distribution of the SiC particles in SZ	• It was found that decreasing the rotational speed and increasing the linear speed led to a decrease in the grain size. • PD was found to be an effective parameter to produce sound surface layer. • PD value was found to be influenced by traverse and rotational speeds and tilt angle.
Mahmoud et al. [26]	Aluminum alloy 1050-H24 and SiC, Al_2O_3 powders	Wear behavior of SMMC	• It was found that addition of reinforcement powder (SiC, Al_2O_3, or mixture) was beneficial in reducing the wear volume loss, especially at relatively low loads.
Alidokht et al. [27]	Aluminum alloy A356, SiC and MoS_2 powders	Microstructure and tribological performance using dry wear tests conducted on pin-on-disk Tribometer	• FSPed A356 displayed higher hardness compared with the as-cast A356. • It was found that both the extent of wear and wear rate were significantly lower in the FSPed A356 and the composite samples as compared with the as-cast A356.

describes some ex situ and in situ nanocomposites fabricated using the FSP technique.

3.1 Ex situ composites

Morisada et al. [33] fabricated multiwalled carbon nanotubes (MWCNTs)/AZ31 surface composites by FSP. Commercially available MWCNTs (outer diameter, 20–50 nm; length, 250 nm) and an AZ31 rolled plate (thickness, 6 mm) were used in this study. The MWCNTs were typically entangled with each other and contain a few graphite granule inclusions. The MWCNTs were filled into a groove (1 mm×2 mm) on the AZ31 plate before the application of FSP. The FSP tool made of SKD61 had a columnar shape (Ø12 mm) with a probe (Ø4 mm; length, 1.8 mm). The probe was inserted into the groove filled with the MWCNTs. Optical microscopy and SEM images were obtained from the surface composites fabricated by the FSP. It was observed that the dispersion of the MWCNTs was related to the travel speed of the rotating tool. A good dispersion of the MWCNTs, which were separated from each other, was obtained for the sample FSPed at 25 mm/min and 1,500 rpm. The FSP with MWCNTs increased the microhardness of the substrates. The maximum microhardness for the composites was 78 HV, while that of the sample treated by the FSP without MWCNTs and the as-received sample was 55 and 41 HV, respectively. The addition of the MWCNTs promoted grain refinement by the FSP. Grains less than 500 nm were easily obtained.

Mg-based nanocomposites were fabricated using FSP by Lee et al. [34]. The AZ61 billets and amorphous SiO_2 nanoparticles with an average diameter of about 20 nm were used. A tool with a pin diameter of 6 mm, a length of 6 mm, a shoulder diameter of 18 mm, and a tilt angle of 2° was used. An advancing speed of 45 mm/min and a rotational speed of 800 rpm were used, which were kept constant in this investigation. The plates were fixed by a fixture, and ambient air cooling was applied. To maintain the entire fixture at the initial temperature (room temperature) after each pass, the back plate of the fixture was designed to contain three cooling channels with cooling water passing through them. To insert the nano-SiO_2 particles, one or two grooves each, 6 mm in depth and 1.25 mm in width, were cut, in which nano-SiO_2 particles were filled to the desired amount before FSP. The groove(s) was aligned with the central line of the rotating pin. The volume fractions of the SiO_2 nanoparticles inserted into the AZ61Mg alloy were calculated to be around 5% and 10% for the one and two deep grooves (1D and 2D), respectively.

Particle clustering was observed, and the size of clustered silica became smaller and smaller with increasing FSP passes. The typical grain sizes of the composites, estimated using both SEM and TEM, with 5% and 10% SiO_2 in volume fraction after four FSP passes were 1.8 and 0.8 μm, respectively. The resulting grain size was significantly refined from the initial grain size of 75 μm for the AZ61 billet. Improvement in mechanical properties was also observed. The yield stress of the FSP composites was improved to 214 MPa in the 1D (one groove) and to 225 MPa in the 2D (two groove) specimens, compared with 140 MPa of the as-received AZ61 billet and 147 MPa of the FSPed AZ61 alloy without silica reinforcement. The ultimate tensile strength (UTS) was also appreciably improved in the composite specimens. The tensile elongation of the 2D and four-pass composites at 350°C reached 350% at 1×10^{-2} s^{-1} and 420% at 1×10^{-1} s^{-1}, clearly exhibiting high strain rate super plasticity.

Microstructures and mechanical properties of the Al/Al_2O_3 surface nanocomposite layer produced by FSP were analyzed by Zarghani et al. [35]. Commercial 6082 Al-extruded bar with a thickness of 7 mm and nanosized Al_2O_3 powder with an average diameter of 50 nm were used as substrate and reinforcement particulates, respectively. The hardened H-13 tool steel pin was 5 mm in diameter, and its length was about 4 mm. The pin rotation was set to be 1,000 rpm, and its advancing speed was 135 mm/min. To insert nanosized Al_2O_3 powder, a groove with a depth and width of 4 and 1 mm, respectively, was machined in which the desired amount of Al_2O_3 powder was filled in. To prevent sputtering of powder and its ejection from groove during the process, the groove's gap initially was closed by means of a tool that only had shoulder and no pin. Samples were subjected to various numbers of passes from one to four, with and without Al_2O_3 powder. After each pass, an ambient air cooling was applied. Optical micrograph of the as-received 6082 Al is shown in Fig. 3a. The grain size of the 6082 Al matrix was refined using the FSP, as shown in Fig. 3b. In comparison with the surface composite layer produced by one FSP pass, the surface composite layer produced by three FSP passes showed a better dispersion of Al_2O_3 particles. There were just a few regions that included the aggregated nanosized Al_2O_3 particles. On the other hand, a good dispersion of nanosized Al_2O_3 particles, which were separated from each other, could be observed for the surface composite layer produced by four FSP passes, as shown in Fig. 3c. As reported by other researchers [36, 37], it was suggested that the grain refinement during FSP was caused by dynamic recrystallization. However, the FSP with the nanosized Al_2O_3 particles more effectively reduced the grain size of the 6082 Al matrix in which some grains were less than 300 nm, as shown in Fig. 3c and 3d. It was considered that the pinning effect by the nanosized Al_2O_3 particles retarded the grain growth of the 6082 Al matrix.

The typical microhardness readings observed by the authors in the central cross-sectional zones of the friction

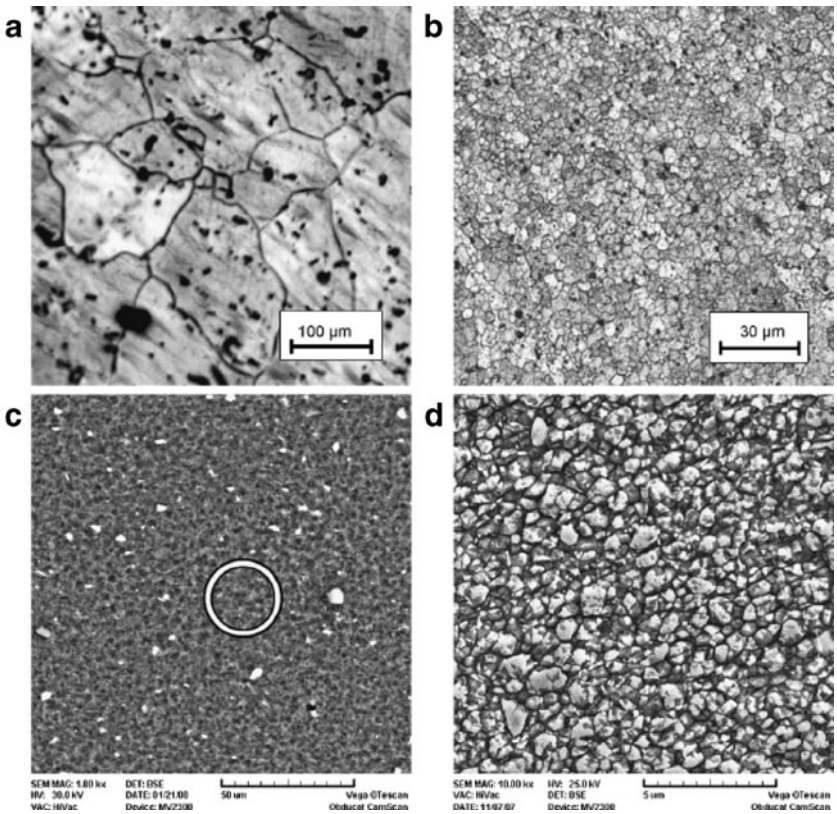

Fig. 3 Optical micrographs showing the grain size of as-received 6082 Al (**a**) and Al 6082 (**b**) after four FSP passes. (**c** and **d**) SEM images showing the microstructure of the Al/Al_2O_3 surface composite layer produced by four FSP passes. Panel (**d**) is enlargement inside a circle for panel (**c**) [35]

stir processed specimens are depicted in Fig. 4a. Almost a three-time increment in the hardness of the parent Al alloy was achieved, especially for the surface composite layer produced by four FSP passes. For the 6082 Al alloy with no alumina powder, after four FSP passes, the microhardness profile showed a general softening and reduction of hardness in the SZ in contrast to that of the as-received Al. The authors compared the kinetics of wear in terms of the weight loss using the specimen as the pin and GCr15 steel as the disk material, as shown in Fig. 4b. The figure showed that the wear weight loss increased with sliding distance. For the as-received Al, the wear rate (weight loss/sliding distance) was low during the initial period of wear, after which it increased, but for the surface nanocomposite layer produced by four FSP passes, the wear rate was roughly constant during sliding time. It was observed that wear resistance against a steel disk was significantly improved (two to three times) in the Al/Al_2O_3 surface nanocomposite layer produced by four FSP passes compared with the as-received Al. The mechanism of wear was a combination of abrasive and adhesive wear. Improved wear resistance of the surface composite layer was attributed to a lower coefficient of friction and an improved hardness

Yang et al. [38] fabricated $AA6061/Al_2O_3$ nanoceramic particle-reinforced composite coating by using FSP. The powder used in this study was the commercially available Al_2O_3 powder (99.9% purity and 50-nm average particle size). Holes with 2 mm in diameter and 2 mm in depth were drilled in the samples using a numerically controlled drilling machine. Al_2O_3 powder mixed with a small amount of methanol was filled into the holes of the aluminum plate. The aluminum plate with preplaced Al_2O_3 particles in the holes was subjected to FSP. During FSP, the linear speed of 203.2 mm/min and the rotational speed of 480 rpm were used. Without interference to each other, FSP was conducted on three paths sequentially on the same plate. The axial force varied from 13.23 to 22.05 kN. Optical microscopic examinations revealed that both the number of FSP passes and axial force had a significant effect on the formation of composite coating. With the increase in FSP passes, plastic deformation within the thermo TMAZ increased, and the clustered or unmixed particles were broken and dispersed into the matrix metal. It was found that the axial force had a significant effect on the formation of aluminum matrix composite zone (AMCZ); that is, a larger axial force makes expanded AMCZ, and as the number of pass increases, the AMCZs were very well bonded to the aluminum alloy substrate. With more FSP passes, the pores became smaller and distributed more evenly. Vickers hardness testing revealed that AMCZ have

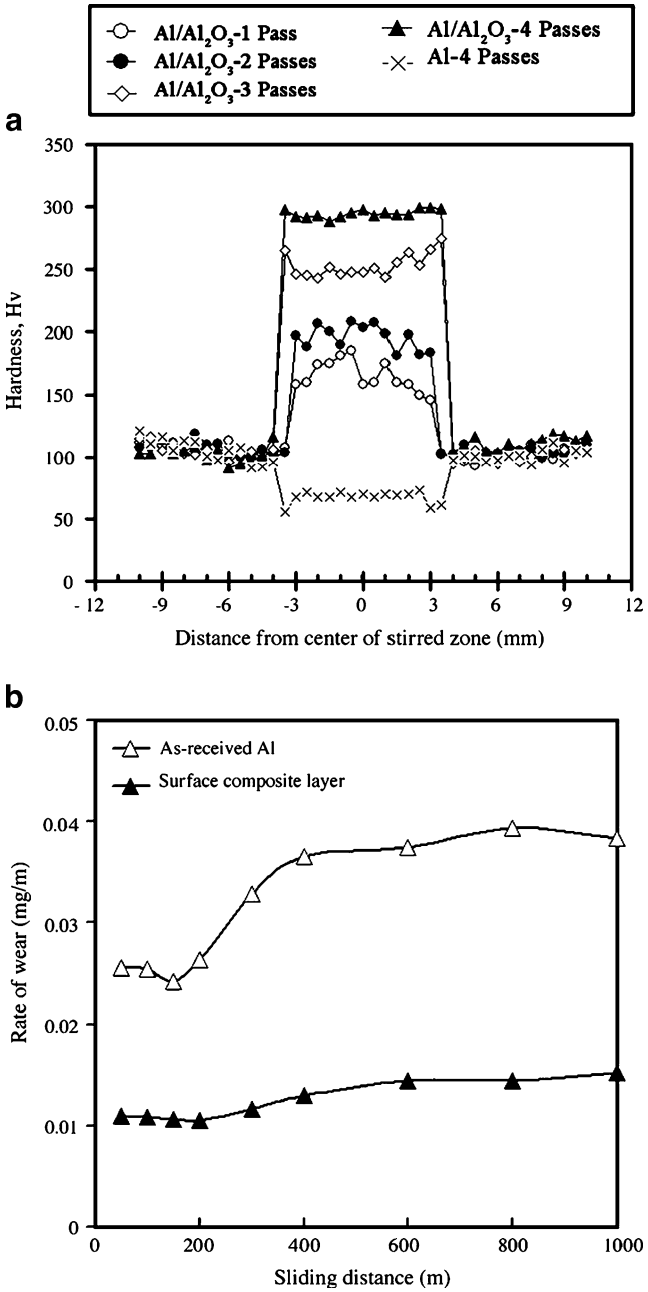

Fig. 4 (**a**) Typical variation of the microhardness HV distributions of the FSPed 6082 Al alloy (no Al_2O_3) and surface composite layers. (**b**) Change in the reduction in pin weight with sliding distance for as-received Al and surface nanocomposite layer produced by four FSP passes [35]

higher hardness values than other zones due to refined grain size via dynamic recrystallization. The lowest hardness was in the heat-affected zone. Measurements on spindle torque indicated that it increased with increasing axial force and became smaller during subsequent passes in multiple-pass FSP.

Nanoceramic particle-reinforced composites were prepared by Sharifitabar et al. [39] via FSP route. Commercial aluminum alloy 5052-H32 rolled plate with 4-mm thickness was used as a starting material. FSP was carried out with a different tool rotation speed to tool travel speed ratios (ω/ν) ranging from 8 to 100 rev/mm and tilting angle of the pin (Φ) ranging from 2.5° to 5° to obtain optimum FSP conditions for fabrication of SZ without macroscopic defects. To insert nanosize Al_2O_3 powder, a groove with a depth and width of 2 and 1 mm was machined out of the work pieces. Then, the desired amount of Al_2O_3 powder was filled in. Samples were subjected to various numbers of passes from one to four, with and without Al_2O_3 powder. The stir zone was found to be defect-free at a tool rotation speed of 1,600 rpm, a tool travel speed of 16 mm/min, and a tilting angle of 5°. In comparison with the surface composite layer produced by one pass, it was found that the surface composite layer produced by four FSP passes showed a good dispersion of nanosized Al_2O_3 particles, which were separated from each other. The size of clusters was reported to be 50–140 nm, with the mean size of 70 nm after four FSP passes, as compared with 200–1,000 nm, with a mean cluster size of 650 nm after the first pass. It was found that the grains of 5052Al matrix were refined by the FSP from an initial 25-μm size to an average grain size of 3.7 to 5.8 μm without powder addition. The average grain size of the stir zone decreased with an increase in the number of FSP pass. It was observed that the multiple-pass FSP with the nanosized Al_2O_3 particles more effectively reduced the grain size of the 5052Al matrix, which ranged from 5.5 to 0.94 μm. The tensile properties of a material, namely tensile strength, YS, and percentage elongation, were also investigated. It was proposed that in the FSP samples produced by one pass, although grain refinement improved tensile and YS, dislocation density decreased and sub-boundaries reduced the tensile strength and, especially, YS of the FSP samples in comparison with the base material. Furthermore, it was observed that an increase in the FSP pass from one to three caused improvement of elongation, especially for the stir zone produced without powder. However, elongation decreased in both samples produced by four passes.

Asadi et al. [40] conducted an experimental investigation on magnesium-base nanocomposite produced by FSP to analyze the effects of particle types and number of FSP passes. The material used was an AZ91 as-cast magnesium alloy with an average grain size of 150 μm. Commercially available SiC and Al_2O_3 particles with average diameter of 30 nm and 99.98 pct purity were used as reinforcements. The reinforcing particles were filled into a groove of 0.8 mm×1.2 mm machined on the AZ91 as-cast plate. The tool rotational and linear speed used was 900 rpm and 63 mm/min, respectively. It was observed during FSP that the alumina particles were agglomerated at different points in the matrix, and alumina clusters were created, uniformly

distributed in the stir zone, whereas SiC particles did not stick together, although the distribution of SiC particles in the Mg matrix was not uniform. Figure 5 shows the average grain size of the specimens produced by different FSP passes and SiC and Al_2O_3 particles. It was found that with an increase in the FSP passes, the average grain size of the SZ decreased. The average hardness of as-cast AZ91 alloy was found to be 63 HV, which increased to a range from 90 to 115 HV with SiC addition and to about 105 HV with Al_2O_3 addition after two passes. It was observed that the UTS and elongation of the one-pass FSPed specimen without powder addition increased from 128 to 194 MPa and from 6 to 18 pct, respectively, compared with the as-cast alloy. The UTS and elongation of the one-pass FSPed specimens with SiC and Al_2O_3 particles was found to reduce as compared with those of the one-pass FSPed specimens without powder addition. It was concluded that almost uniform and separately distributed nanoparticles and very fine grains in the eight-pass FSPed specimens improved the strength and elongation significantly as compared with the one-pass FSPed specimens. The distributed SiC particles in the AZ91 matrix acted as barriers to wear and prevented severe adhesive wear, consequently slowing the wear rate. The dominant wear mechanism in this specimen was found to be abrasive wear. However, the presence of coarse alumina clusters (~7 μm) and their low integrity with the AZ91 matrix caused delamination of substrate layers of the matrix. Uniform distribution of reinforcing particles gave the eight-pass FSPed specimens a uniform worn surface with mild abrasive wear mechanism. In these specimens, delamination of the substrate layers or adhesive wear was diminished.

Mazaheri et al. [41] developed A356/Al_2O_3 surface nanocomposite by FSP. The specimens used for the FSP

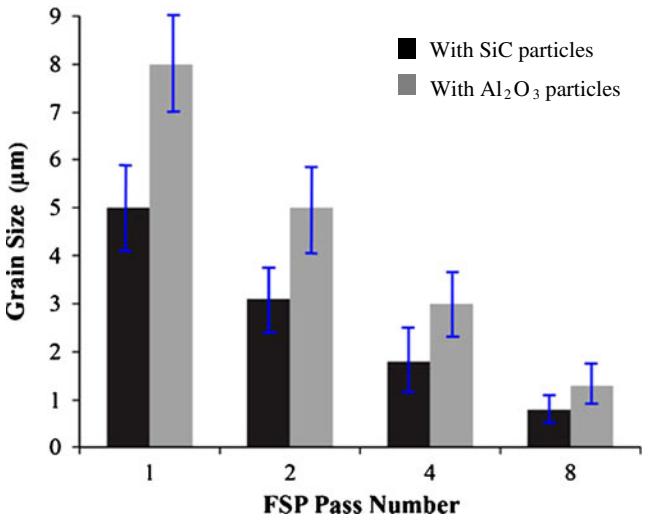

Fig. 5 Average grain size in the specimens produced by several FSP passes and SiC and Al_2O_3 particles [40]

experiments were A356-T6 10 mm×50 mm×250 mm bars. The A356 chips and Al_2O_3 powder particles were mixed to achieve A356–5 vol.% Al_2O_3 composition. A356–Al_2O_3 composite powder was prepared by 12-h ball milling of A356 machining chips and nanosized as well as microsized Al_2O_3 powder. The composite powders were deposited onto the grit blasted A356-T6 substrates by high velocity oxy fuel (HVOF) spraying. Then, plates with preplaced composite coatings were subjected to FSP. The FSP tool was made of H13 steel. In all FSP experiments, tool rotation speed, linear speed, and tilt of the spindle toward trailing direction were kept constant, with values being 1,600 rpm, 200 mm min^{-1}, and 2°, respectively. The surface composite layers were found to be very well bonded to the aluminum alloy substrates, and no defects were visible. The hardness profile along the cross-section of the FSPed samples was also determined by a microhardness test using a Vickers indenter at a load of 100 g and a dwell time of 5 s. The average microhardness values for A356–μAl_2O_3 and A356–nAl_2O_3 surface composites were about 90 and 110 HV, respectively, which was found to be higher than that of the as-received and FSPed A356-T6. The microhardness of the surface layer of aluminum substrates was observed to increase significantly as the Al_2O_3 particle size was decreased. Al_2O_3 particles also increased the resistance of aluminum matrix to indentation.

3.2 In situ composites

Hsu et al. [42] fabricated Al–Al_3Ti in situ nanocomposites using FSP. The starting materials used were aluminum powder and titanium powder. Titanium contents of 5, 10, and 15 at.% were premixed with aluminum powder (denoted Al–5Ti, Al–10Ti, and Al–15Ti). Counterclockwise tool rotation with a speed of 700 and 1,400 rpm and a linear speed of 45 mm/min was used along the long axis of the billet. Multiple FSP passes were applied to the billet to enhance the Al–Ti reaction. For multiple FSPs, the pin tool was moved along the same line, and the FSP pass was applied after the work piece had been cooled from the previous FSP pass.

X-ray diffraction (XRD) was used to identify the phases present in the SZ of specimens during FSP. The diffraction patterns showed that Ti reacted with Al to form Al_3Ti, but some unreacted Ti remained after four FSP passes. The microstructure of FSP specimens was observed using SEM/backscattered electron image. The fine particles of micrometer size were pure Ti, which were verified using energy dispersive spectroscopy, and the very fine particles (<100 nm) were Al_3Ti particles, which were uniformly dispersed in the Al matrix. After FSP, the average size of Ti particles was refined from 40 μm to about 1–5 μm. For Al–15Ti after four FSP passes, the volume fraction of Al_3Ti

was close to 0.5, which resulted in a hardness value of 200 HV. It was concluded that Al_3Ti particle size was affected by both the Ti content and the FSP parameters. It increased with increasing tool rotation speed and Ti content, since a higher temperature was obtained from a higher tool rotation speed and a higher Ti content. In addition, the Al_3Ti particle size also increased with increasing number of FSP passes, which was suggested to be the result of a longer time exposed at elevated temperature with increasing FSP passes. The Young's modulus of the Al–Al_3Ti composites increased significantly with increasing volume fraction of Al_3Ti. For an Al–15Ti material, the Young's modulus reached 114 GPa, which is 63% higher than that of Al. The high strength of these FSP Al–Al_3Ti composites was attributed to the presence of a large volume fraction of nanometer-sized Al_3Ti particles, which contributed significantly to the strength through the Orowan mechanism, as well as the ultrafine grain size of the Al matrix.

Hsu et al. [43] investigated the ultrafine-grained Al–Al_2Cu composite produced in situ by FSP. The starting materials used were pure aluminum powder and pure copper powder. The premixed Al–15Cu alloy powders were cold compacted to a small billet in a steel die. A counterclockwise tool rotation speed of 700 rpm and a linear speed of 45 mm/min were used. To obtain a fully dense solid from a powder compact, two FSP passes were applied to the billet. XRD was utilized to identify the phases present in the specimens. SEM was used to study the distribution of second-phase particles. The Vickers microhardness was measured with 300 g load for 15 s. Mechanical properties of specimens machined from the SZ were evaluated at an initial strain rate of 1×10^{-3} s^{-1}. It was revealed that the FSP resulted in a significant increase in hardness from 80 HV in base metal to 160±14 HV in the SZ. In addition, the hardness distribution within the SZ was not symmetric with respect to the tool rotation axis. The microstructure of the as-sintered material was revealed by the backscattered electron image. It indicated that Cu-rich particles were homogenously distributed in the aluminum matrix after FSP. TEM images showed that the grain sizes of both phases were refined to be below 1–2 μm. Some of the dispersed particles were found to be smaller than 100 nm. The Al_2Cu grains were also confirmed by EDX analysis, which showed that the Cu-rich grains contained 32±6 at.% Cu. The composite possessed enhanced Young's modulus (88±8 GPa) and good compressive strength (450 MPa YS and 650 MPa ultimate strength) with reasonable good compressive ductility (0.15 failure strain).

Zhang et al. [44] produced in situ Al_3Ti and Al_2O_3 nanoparticle-reinforced Al composites by FSP in an Al–TiO_2 system. Commercial pure Al powder and TiO_2 powder were used. The volume fraction of reinforcements (Al_3Ti+Al_2O_3) was 25%. The as-mixed powders were hot pressed into billets and then hot forged at 723 K into disk plates of 10 mm in thickness. The plates were subjected to four-pass FSP with 100% overlapping in air (defined as FSP-air). Furthermore, some FSP-air samples were subjected to additional two-pass FSP with 100% overlapping in the flowing water. The XRD results indicated that four-pass FSP induced the reaction between Al and TiO_2, forming Al_3Ti, α-Al_2O_3, and a small quantity of TiO. In this study, Al_3Ti and α-Al_2O_3 formed within only a few seconds during FSP. The accelerated forming of Al_3Ti and α-Al_2O_3 was attributed to severe plastic deformation during FSP, which broke up the oxide film on the Al particles and caused intimate contact between Al and TiO_2, and then reduced the diffusion distance of elements. Second, the high density of dislocations produced by severe plastic deformation during FSP not only provided the nucleation sites of Al_3Ti and α-Al_2O_3 but also assisted in growth of an embryo beyond the critical size by providing a diffusion pipe. The grain sizes in the FSP-air and FSP-water samples were determined, by averaging the sizes of about 100 grains, to be 1,285 and 602 nm, respectively. This indicated that rapid cooling after FSP effectively inhibited the growth of the recrystallized grains. The YS, UTS, and uniform elongation of the FSP-air sample was found to be 210 MPa, 286 MPa, and 11.5%, respectively. By comparison, the FSP-water sample exhibited much higher YS and UTS due to finer grain size, whereas the uniform elongation decreased to 6.8%, which was still above the critical ductility (5%) required for many structural applications.

The effect of FSP on microstructure and properties of Al–TiC in situ composites was investigated by Bauri et al. [45]. K_2TiF_6 salt and graphite powder with average particle size of 50 μm were used as precursor materials to form the TiC particles in situ in the aluminum melt. Commercially pure Al was melted in a resistance-heated furnace under an inert gas (argon) atmosphere. When the temperature reached to 1,200°C, K_2TiF_6 and graphite mixture was added with the help of a plunger. The melt was held for 60 min for the reaction to complete. The as-cast composite plate was machined to a thickness of 10 mm for FSP. A rotational speed of 1,000 rpm and a traverse speed of 60 mm/min were used for FSP. Metallurgical characterization was done using electron back scatter diffraction (EBSD), field emission gun (FEG-SEM), TEM, and XRD and mechanical characterization using microhardness test and tensile tests. It was found that the TiC particles were segregated at the grain boundaries in the as-cast material, which were nearly uniformly distributed within the matrix after two-pass FSP. The average grain size of the FSPed composites after single and double pass was found to be 9 and 4 μm, respectively, as compared with

Table 2 Summary of the investigations on nanocomposite fabrication using FSP

Investigator name	Material investigated	Characteristic studied	Prominent results
Morisada et al. [33]	Magnesium alloy AZ31 and MWCNTs	Effect of processing parameters on microstructure, grain refinement, and microhardness	• The addition of the MWCNTs promoted grain refinement by the FSP. • Good dispersion of the MWCNTs was obtained for the sample FSPed at 25 mm/min and 1,500 rpm. • The FSP with MWCNTs increased the microhardness of the substrates
Lee et al. [34]	Magnesium alloy AZ61 and SiO_2 nanoparticles	Microstructural observations of the nanocomposite formed and mechanical properties	• The yield stress of the FSP composites was improved to 214 MPa in the 1D (one groove) and to 225 MPa in the 2D (two groove) specimens, compared with 140 MPa of the as-received AZ61 billet and 147 MPa of the FSPed AZ61 alloy without silica reinforcement.
Zarghani et al. [35]	Aluminum alloy 6082 and Al_2O_3 powder	Grain refinement by multipass FSP, microhardness, and wear behavior of surface composite formed	• The surface composite layer produced by three FSP passes showed a better dispersion of Al_2O_3 particles. • Almost a three-time increment of the hardness of the parent Al alloy was achieved. • It was observed that wear resistance against a steel disk was significantly improved (two to three times) in the Al/Al_2O_3 surface nanocomposite layer produced by four FSP passes compared with the as-received Al.
Yang et al. [38]	Aluminum alloy 6061 and nano-Al_2O_3 particle	Effect of axial force and multipass, hardness values in the composite zone formed	• Larger axial force makes the expanded AMCZ and bonding of AMCZ increases with number of passes. • Pores became smaller and more distributed. • FSZ had higher hardness values than other zones due to refined grain size via dynamic recrystallization.
Sharifitabar et al. [39]	Aluminum alloy 5052-H32, Al_2O_3 powder	Grain size refinement and elongation	• Multiple-pass FSP with the nanosized Al_2O_3 particles more effectively reduced the grain size of the 5052Al matrix, which ranged from 5.5 to 0.94 μm. • It was observed that an increase in the FSP pass from one to three caused improvement of elongation, especially for stir zone produced without powder. However, elongation decreased in both samples produced by four passes.
Asadi et al. [40]	Magnesium alloy AZ91, SiC and Al_2O_3 powders	Microhardness of the composite formed	• It was found that with an increase in FSP passes, the average grain size of the SZ decreased. • The average hardness of as-cast AZ91 alloy was found to be 63 HV, which increased to a range from 90 to115 HV with SiC addition and about 105 HV with Al_2O_3 addition after two passes.
Mazaheri et al. [41]	Aluminum ally A356 and Al_2O_3 powder	Vickers microhardness	• The average microhardness values for A356–μAl_2O_3 and A356–nAl_2O_3 surface composites were about 90 and 110 HV, respectively
Hsu et al. [42]	Aluminum and titanium powder	Microstructural observations and mechanical properties	• Very fine Al_3Ti particles less than 100 nm in size were formed. • It was concluded that the Al_3Ti particle size was affected by both the Ti content and the FSP parameters. • The Young's modulus of the Al–Al_3Ti composites increased significantly with increasing volume fraction of Al_3Ti.
Hsu et al. [43]	Aluminum and copper powder	Microstructural observations and mechanical properties	• Particles less than 100 nm were formed. • The composite possessed enhanced Young's modulus and good strength with reasonable good compressive ductility.
Zhang et al. [44]	Commercial pure Al powder and TiO_2 powder	YS, UTS, and uniform elongation	• FSP-water sample exhibited much higher YS and UTS as compared with FSP-air sample due to finer grain size. • Uniform elongation decreased to 6.8%.
Bauri et al. [45].	Commercially pure Al, K_2TiF_6 salt and	Microhardness and tensile tests of the composite formed	• Microhardness after second pass increased to 58 VHN from 38 VHN.

Table 2 (continued)

Investigator name	Material investigated	Characteristic studied	Prominent results
	graphite powder		• Strength increased by 17% after-single pass and 40% after double-pass FSP.
Barmouz et al. [46]	HDPE Rigdex HD 5218 EA and nanoclay particles	Microhardness of the composite formed	• A 62% increase was observed in the case of microhardness values of the nanocomposites prepared by the FSP method.

48 μm for the as-cast material. It was observed that the hardness increased significantly after FSP. The hardness after first and second FSP passes was found to be 48 and 58 vickers hardness number (VHN), respectively compared with 38 VHN for the as-cast composite. The improved homogeneity of particle distribution after FSP gave rise to a more effective dispersion hardening. A considerable improvement in the strength was also observed after FSP. The 0.2% proof stress after a single-pass FSP (103 MPa) increased by 17%, and after a double-pass FSP , it increased by 40% (123 MPa) compared with the as-cast composite (88 MPa). Similarly, the UTS also improved substantially after FSP. This improvement in mechanical properties was obtained without compromising the ductility.

Barmouz et al. [46] produced polymer nanocomposites by in situ dispersion of clay particles via FSP. The materials used in this study were high-density polyethylene (HDPE) Rigdex HD 5218 EA and nanoclay Cloisite 20A. Nanoclay particles were contrived in a groove with a dimension of 1 mm×1 mm in the middle of the samples. FSP tools were made of hot-working steel. Dispersion of nanoclay particles in the polymer matrix was examined by TEM. Significant enhancement in storage modulus (G) values was observed upon the addition of nanoclay into the parent HDPE using the melt mixing method. The FSPed nanocomposite showed further increment in the G value. Storage modulus was found to increase as the traverse speed of the tool increased, which could be ascribed to the reinforcing effect of clay particles and a high level of delamination of clay layers. According to the results, a 62% increase was observed in the case of microhardness values of the nanocomposites prepared by the FSP method, whereas the sample that was prepared by internal batch mixer showed a 22% enhancement in microhardness values. Microhardness value was observed to increase with an increase in the tool rotational speed.

Summary of the investigations on nanocomposite fabrication using FSP is given in Table 2.

4 Summary and discussion

FSP has successfully evolved as a composite fabrication process. The major challenge in generation of ex situ composites wherein the reinforcement particles are externally added to the material is the agglomeration of extremely fine reinforcing particles. The large plastic strain in FSP can shear the metal powders and break the oxide film surrounding reinforcement particles, which causes intimate contact between the matrix and the reinforcement and promotes the reaction. The tendency of particle agglomeration can be significantly reduced by appropriate selection of an FSP tool shoulder diameter, which is mainly responsible for the generation of frictional and shear force. Pretreatment of the reinforcements for improving wettability, together with multipass FSP, offers another alternative for uniform distribution of the very fine reinforcing particles in the FSP nugget zone. The selection of optimum FSP parameters is of utmost importance for the production of a sound composite zone using this technology. The amount of heat generation during FSP is a decisive issue to produce a defect-free FSPed zone. Small friction coefficient between the tool shoulder and the work piece surface is not sufficient to produce enough heat to make the material soft enough, and as a result, the brittle fracture can occur. On the other hand, inordinate increase in the friction coefficient may cause the work piece to stick to the tool and form the defects. Extremely fine reinforcements act as pinning sites and result in refining the grain structure even more than the FSPed zone without reinforcements, thereby significantly improving the overall properties of the material in the form of enhanced microhardness, greater Young's modulus, and strength. Furthermore, the high plastic stain imposed on the work piece during FSP not only promotes mixing but also increases the diffusion rate of elements, thereby accelerating the reaction between material constituent elements. Otherwise, FSP can also provide elevated temperature to facilitate the formation of intermetallic phase in situ and accelerate the reaction between material constituent elements.

Thus, the successful application of the FSP technique in generating surface and bulk composites firmly establishes it in the field of composite manufacturing. Further research efforts in this field and better understanding of the process characteristics can pave the way for the commercial success of this technology as well.

References

1. Zweben C (2002) Metal matrix composites, ceramic matrix composites, carbon matrix composites and thermally conductive polymers matrix composites. In: Harper CA (ed) Handbook of plastics, elastomers, and composites, 4th edn. McGraw Hill, New York, p 321
2. Mangalgiri PD (1999) Composite materials for aerospace applications. J Bull Mater Sci 22(3):657–664
3. Lloyd DJ (1994) Int Mater Rev 39:1–23
4. Tjong SC, Ma ZY (2000) Mater Sci Eng R 29:49–113
5. Thomas WM, Nicholas ED, Needham JC, Church MG, Templesmith P, Dawes CJ (1991) The Welding Institute, TWI, International Patent Application No. PCT/GB92/02203 and GB Patent Application No. 9125978.8
6. Mishra RS, Mahoney MW, McFadden SX, Mara NA, Mukherjee AK (2000) Scr Mater 42:163–168
7. Ma ZY, Mishra RS, Mahoney MW (2002) Acta Mater 50:4419–4430
8. Kwon YJ, Shigematsu I, Saito N (2003) Scr Mater 49:785–789
9. Rhodes CG, Mahoney MW, Bingel WH, Spurling RA, Bampton CC (1997) Scr Mater 36:69–75
10. Chang CI, Lee CJ, Huang JC (2004) Scr Mater 51:509–514
11. Su JQ, Nelson TW, Sterling CJ (2003) J Mater Res 18:1757–1760
12. Saravanan RA, Surappa MK (2000) Mater Sci Eng, A 276:108–116
13. Hu L, Wang E (2000) Mater Sci Eng, A 278:267–271
14. Han BQ, Dunand DC (2000) Mater Sci Eng, A 277:297–304
15. Lee DM, Suh BK, Kim BG, Lee JS, Lee CH (1997) Mater Sci Technol 13:590–595
16. Mishra RS, Ma ZY (2005) Mater Sci Eng R 50:1–78
17. Hsu CJ, Kao PW, Ho NJ (2005) Scr Mater 53:341–345
18. Lee IS, Kao PW, Ho NJ (2008) Intermetallic 16:1104–1108
19. Clyne TW, Withers PJ (1993) An introduction to metal matrix composites. Cambridge University Press, Cambridge
20. El-Danaf EA, El-Rayes MM, Soliman SM (2010) Friction stir processing: an effective technique to refine grain structure and enhance ductility. Mater Des 31:1231–1236
21. Wang W, Shi Q, Liu P, Li H, Li T (2009) A novel way to produce bulk SiCp reinforced aluminum metal matrix composites by friction stir processing. J Mater Process Technol 209:2099–2103
22. Lim DK, Shibayanagi T, Gerlicha AP (2009) Synthesis of multi-walled CNT reinforced aluminum alloy composite via friction stir processing. Mater Sci Eng, A 507:194–199
23. Ke L, Huang C, Xing Li, Huang K Al–Ni intermetallic composites produced in situ by friction stir processing. J. of Alloys and Compounds 503(2):494–499
24. Dixit M, Newkirk WJ, Mishra RS (2007) Properties of friction stir-processed Al 1100–NiTi composite. Scr Mater 56:541–544
25. Asadi P, Faraji G, Besharati MK (2010) Producing of AZ91/SiC composite by friction stir processing. Int J Adv Manuf Technol 51:247–260
26. Mahmouda ERI, Takahashi M, Shibayanagi T, Ikeuchi K (2010) Wear characteristics of surface-hybrid-MMCs layer fabricated on aluminum plate by friction stir processing. Wear 268:1111–1121
27. Alidokht SA, Abdollah-zadeh A, Soleymani S, Assadi H (2011) Microstructure and tribological performance of an aluminum alloy based hybrid composite produced by friction stir processing. Mater Des 32:2727–2733
28. Breuer O, Sundararaj U (2004) Big returns from small fibers: a review of polymer/carbon nanotube composites. Polymer Compos 25(6):630–645
29. Thostenson ET, Ren Z, Chou TW (2001) Advances in the science and technology of carbon nanotubes and their composites: a review. Compos Sci Technol 61(13):1899–1912
30. Lau KT, Hui D (2002) The revolutionary creation of new advanced materials—carbon nano-tube composites. Compos Part B Eng 33(4):263–277
31. Gojny FH, Wichmann MHG, Fiedler B, Bauhofer W, Schulte K (2005) Influence of nano-modification on the mechanical and electrical properties of conventional fibre-reinforced composites. Compos Part A Appl Sci Manuf 36(11):1525–1535
32. Gou J, Braint SO, Gu H, Song G (2006) Damping augmentation of nanocomposites using carbon nanofiber paper. J Nanomater 2006:1–7
33. Morisada Y, Fujii H, Nagaoka T, Fukusumim M (2006) MWCNTs/AZ31 surface composites fabricated by friction stir processing. Mater Sci Eng, A 419:344–348
34. Lee CJ, Huang JC, Hsieh PJ (2006) Mg based nano-composites fabricated by friction stir processing. Scr Mater 54:1415–1420
35. Zarghani SA, Kashani-Bozorg SF, Zarei-Hanzaki A (2009) Microstructures and mechanical properties of Al/Al_2O_3 surface nano-composite layer produced by friction stir processing. Mater Sci Eng, A 500:84–91
36. Java KV, Sankaran KK, Rushau JJ (2000) Metall Mater Trans A 31A:2181–2188
37. Sato YS, Kokawa H (2001) Metall Mater Trans A 32A:3023–3031
38. Yang M, Xu C, Wu C, Lin K, Chao Y, An L (2010) Fabrication of $AA6061/Al_2O_3$ nano ceramic particle reinforced composite coating by using friction stir processing. J Mater Sci 45(16):4431–4438
39. Sharifitabar M, Sarani A, Khorshahian S, Shafiee Afarani M (2011) Fabrication of $5052Al/Al_2O_3$ nanoceramic particle reinforced composite via friction stir processing route. Mater Des 32:4164–4172
40. Asadi P, Faraji G, Masoumi A, Besharati givi MK (2011) Experimental investigation of magnesium-base nanocomposite produced by friction stir processing: effects of particle types and number of friction stir processing passes. Metall Mater Trans A. doi:10.1007/s11661-011-0698-8
41. Mazaheri Y, Karimzadeh F, Enayati MH (2011) A novel technique for development of $A356/Al_2O_3$ surface nanocomposite by friction stir processing. J Mater Process Technol. doi:10.1016/j.jmatprotec.2011.04.015
42. Hsu CJ, Chang CY, Kao PW, Ho NJ, Chang CP (2006) $Al–Al_3Ti$ nanocomposites produced in situ by friction stir processing. Acta Mater 54:5241–5249
43. Hsu CJ, Kao PW, Ho NJ (2005) Ultrafine-grained $Al–Al_2Cu$ composite produced in situ by friction stir processing. Scr Mater 53:341–345
44. Zhang Q, Xiao BL, Wang QZ, Ma ZY (2011) In situ Al_3Ti and Al_2O_3 nanoparticles reinforced Al composites produced by friction stir processing in an $Al–TiO_2$ system. Mater Lett 65:2070–2072
45. Bauri R, Yadav D, Suhas G (2011) Effect of friction stir processing (FSP) on microstructure and properties of Al–TiC in situ composite. Mater Sci Eng, A 528:4732–4739
46. Barmouza M, Seyfib J, Givia MKB, Hejazic I, Davachi SM (2011) A novel approach for producing polymer nanocomposites by in-situ dispersion of clay particles via friction stir processing. Mater Sci Eng, A 528:3003–3006